THE JOURNAL OF BIOLOGICAL CHEMISTRY VOL. 286, NO. 50, pp. 43417–43428, December 16, 2011

Endogenous Myoglobin in Breast Cancer Is Hypoxia-inducible by Alternative Transcription and Functions to Impair Mitochondrial Activity

A ROLE IN TUMOR SUPPRESSION?[*] [S]

Received for publication, February 4, 2011, and in revised form, September 6, 2011 Published, JBC Papers in Press, September 19, 2011, DOI 10.1074/jbc.M111.227553

Glen Kristiansen[‡1], Junmin Hu[§], Daniela Wichmann[§], Daniel P. Stiehl[¶], Michael Rose[‖], Josefine Gerhardt[**], Annette Bohnert[**], Anette ten Haaf[‖], Holger Moch[**], James Raleigh[‡‡], Mahesh A. Varia[‡‡], Patrick Subarsky[§§], Francesca M. Scandurra[§§], Erich Gnaiger[§§], Eva Gleixner[¶¶], Anne Bicker[¶¶], Max Gassmann[§], Thomas Hankeln[¶¶], Edgar Dahl[‖2], and Thomas A. Gorr[§‖‖2]

From the [‡]Institute of Pathology, University Hospital Bonn, 53127 Bonn, Germany, the [§]Institute of Veterinary Physiology, Vetsuisse Faculty, Zurich Center for Integrative Human Physiology, University of Zurich, 8057 Zurich, Switzerland, the [¶]Institute of Physiology, University of Zurich, 8057 Zurich, Switzerland, the [‖]Institute of Pathology, University Hospital of the RWTH, 52074 Aachen, Germany, the [**]Institute of Surgical Pathology, University Hospital Zurich, 8091 Zurich, Switzerland, the [‡‡]University of North Carolina School of Medicine, Chapel Hill, North Carolina 19044, the [§§]D. Swarovski Research Laboratory, Department of Visceral, Transplant and Thoracic Surgery, Medical University of Innsbruck, 6020 Innsbruck, Austria, the [¶¶]Institute of Molecular Genetics, Johannes Gutenberg University Mainz, 55099 Mainz, Germany, and the [‖‖]Center for Pediatrics and Adolescent Medicine, University Medical Center Freiburg, 79106 Freiburg, Germany

Background: The role of MB in tumors cells is yet unclear.
Results: MB is induced by hypoxia in breast cancer cell lines, possibly by an alternative transcription start site. Knockdown of MB in breast cancer cells is functionally relevant and significantly alters cellular respiration.
Conclusion: MB might impair mitochondria in hypoxic cancer cells.
Significance: MB might have tumor-suppressive functions, not described so far.

Recently, immunohistochemical analysis of myoglobin (MB) in human breast cancer specimens has revealed a surprisingly widespread expression of MB in this nonmuscle context. The positive correlation with hypoxia-inducible factor 2α (HIF-2α) and carbonic anhydrase IX suggested that oxygen regulates myoglobin expression in breast carcinomas. Here, we report that MB mRNA and protein levels are robustly induced by prolonged hypoxia in breast cancer cell lines, in part via HIF-1/2-dependent transactivation. The hypoxia-induced *MB* mRNA originated from a novel alternative transcription start site 6 kb upstream of the ATG codon. MB regulation in normal and tumor tissue may thus be fundamentally different. Functionally, the knockdown of MB in MDA-MB468 breast cancer cells resulted in an unexpected increase of O_2 uptake and elevated activities of mitochondrial enzymes during hypoxia. Silencing of *MB* transcription attenuated proliferation rates and motility capacities of hypoxic cancer cells and, surprisingly, also fully oxygenated breast cancer cells. Endogenous MB in cancer cells is apparently involved in controlling oxidative cell energy metabolism, contrary to earlier findings on mouse heart, where the targeted disruption of the *Mb* gene did not effect myocardial energetics and O_2 consumption. This control function of MB seemingly impacts mitochondria and influences cell proliferation and motility, but it does so in ways *not* directly related to the facilitated diffusion or storage of O_2. Hypothetically, the mitochondrion-impairing role of MB in hypoxic cancer cells is part of a novel tumor-suppressive function.

Mammalian myoglobin (MB)[3] is a cytoplasmic heme-containing respiratory protein of cardiac myocytes and oxidative type I/IIa skeletal muscle fibers. In striated human muscles, MB occurs at concentrations of ~200–300 μM. Here, the monomeric globin is widely accepted to function as a temporary "store" for oxygen, able to buffer short phases of exercise-induced increases in O_2 flux during which it supplies the gas to mitochondria (2). Another more controversially discussed role of MB is the facilitation of O_2 diffusion within muscle cells (3, 4). *Mb* knock-out ($Mb^{-/-}$) mice exhibited normal development and exercise capacity and showed no signs of compromised cardiac energetics due to multiple systemic compensa-

* This work was supported in part by grants from the Swiss National Science Foundation (to M. G.), a grant from the Faculty of Medicine, RWTH Aachen (START network) (to E. D.), and by contributions from K-Regio Project MitoCom Tyrol (to E. G.). Parts of this paper have been presented at the International Congress of Respiratory Science, August 9–13, 2009, Bad Honnef, Germany.
[S] The on-line version of this article (available at http://www.jbc.org) contains supplemental Figs. S1 and S2.
[1] To whom correspondence should be addressed: Institute of Pathology, University Hospital Bonn (UKB), Sigmund-Freud-Str. 25, 53127 Bonn, Germany. Tel.: 49-228-287-15375; Fax: 49-228-287-15030; E-mail: glen.kristiansen@ukb.uni-bonn.de.
[2] Both authors should be considered senior authors.

[3] The abbreviations used are: MB, myoglobin; DCIS, ductal carcinoma *in situ*; MTT, dimethylthiazolyldiphenyltetrazolium bromide; ERα, estrogen receptor α; HIF, hypoxia-inducible factor; LoF, loss-of-function; ROX, residual O_2 consumption; ETS, electron transfer capacity; HRE, hypoxia-response element; scr, scrambled; si, silencing; KD, knockdown; FCCP, carbonyl cyanide-4-(trifluoromethoxy)phenylhydrazone; CAIX, carbonic anhydrase IX.

tions (1, 5). The fact that these compensations (*i.e.* increases in capillarity, coronary flow, coronary reserve, and hematocrit) acted in concert to reduce the diffusion path length for O_2 between capillaries and the mitochondria strongly argued for the importance of Mb with regard to the delivery of O_2. Follow-up studies stressed the additional relevance of functional Mb in maintaining nitric oxide (NO) homeostasis in muscle through either scavenging (6) or producing the NO molecule (7). Beyond transporting/storing diatomic gaseous ligands (O_2, NO), the physiological facets of MB might also include synthesis of peroxides (8), scavenging of reactive O_2 species (9), and binding of fatty acids (10, 11). However, the oxygenation-support function of MB in myocytes is widely accepted and further underscored by the O_2 responsiveness of the *MB* gene.

Expression of MB was found up-regulated in oxidative myofibers of humans in response to exposure to high altitudes (1) or intense endurance training under reduced O_2 pressures (2, 12–14). Whether or not HIF-1, the chief transducer of falling O_2 partial pressure (pO_2) at the level of DNA, is responsible for this up-regulated gene activity in humans remains a matter of debate. Although HIF-1 signaling is known to be stimulated in muscle by exercise, with or without hypoxia, and in response to muscular stretching (13, 15, 16), conserved HIF-binding hypoxia-response elements (HREs) are lacking in the standard promoter of the *MB* gene (17). Yet in striated muscles of mice, HIF-1 has been implicated in the induction of Mb expression during chronic hypoxia (18). Contrary to that, when Kanatous *et al.* (19) subjected mice to week-long hypoxia in the presence or absence of exercise-induced stimuli, they observed in the working heart, but not in skeletal muscles, a reprogrammed calcium signaling that triggered the subsequent increase of *Mb* gene expression independently from HIF-1.

The doctrine that MB is solely a product of striated muscles, lost ground in 2006, when Fraser *et al.* (20) demonstrated that the hypoxia-tolerant common carp (*Cyprinus carpio*) has Mb not only in muscle but also in other metabolically active tissues, including liver, brain, and gills. More than that, the carp generates not one but two Mbs from distinct genes (*Mb-1* and *Mb-2*) of which one (*Mb-1*) was robustly induced as transcript and protein in all nonmuscle tissues upon exposure of the fish to day-long O_2 deprivation. Both proteins also occur in nonmuscle tissues of the closely related and equally hypoxia-tolerant goldfish (*Carassius auratus*) (21). MB is also present in smooth muscles of birds (*i.e.* the gizzard (22)) and humans (*i.e.* rectal sphincter (23)). In addition, low levels of MB are variably detected in different malignant tumors of human subjects, including breast cancer (24–28), but the physiological function of endogenous MB in cancer cells remains a mystery.

We recently conducted the first comprehensive analysis of MB expression in a large and representative cohort of human breast cancer (29). Subsequently, we documented other globins, namely hemoglobin and cytoglobin, to also be expressed in human breast cancer and have begun to unravel their functional implications in this setting (30). In this study, we focus on the mechanistic details of human MB expression in malignant breast carcinomas and cancer cell lines. Carcinoma-expressed MB was found strongly associated with known marker genes of hypoxia. Cultured human breast cancer cells, but not healthy breast epithelial cells, robustly induce the expression of MB mRNA and protein when challenged by prolonged hypoxia. This induction by hypoxia requires, to a large extent, transactivation by HIF-1 and -2. Transcription of the *MB* gene in breast cancer cells is launched via a novel alternative start site 6 kb upstream of the translation initiation codon. In line with the hypoxic activation of the gene, the alternative start site is flanked by a functional HRE. RNA interference-mediated silencing of MB function suggested that the hemoprotein is involved in regulating respiratory, proliferative, and motility activities in oxygenated and hypoxic breast cancer cells. Accordingly, MB in breast cancer might aid in adjusting the proliferative and oxidative capacities of the cells during prolonged hypoxia. In addition, MB promotes the growth of fully oxygenated breast cancer cells, perhaps through controlling fatty acid homeostasis and lipogenesis (29).

EXPERIMENTAL PROCEDURES

Cell Lines and Hypoxia Exposures

Human mammary epithelial cell line MCF12A and the breast cancerous cell lines MDA-MB231, MDA-MB468, and MCF7 were obtained from ATCC (Manassas, VA) and cultured as recommended. Culture atmospheres included the following: normoxia = ventilated room air in water-saturated 5% CO_2 atmosphere = 141.6 mm Hg or 18.6% O_2 (sea level, 37 °C); hypoxia = water-saturated 1% O_2, 5% CO_2/balance N_2 atmosphere at 37 °C. We used Hera cell 240 incubators (MultiTemp Scientific AG, Kloten, Switzerland), an IG150 incubator (Jouan, Unterhaching), a CB 53 CO_2 incubator (Binder), a polymer Coy glove box (Coy Laboratory Products Inc., Grass Lake, MI), or Invivo$_2$ 400 hypoxia workstations (Ruskinn Technology Ltd., Leeds, UK) for hypoxic exposures.

Quantitative Real Time Reverse Transcription-PCR

Quantitative PCR experiments used the ABI Prism 7500 Fast SDS (Applied Biosystems, Darmstadt, Germany) and primers given in Table 1 (see Ref. 31 for details). Mean (±S.D.) expression levels of standard (NM_005368, *MB-S*) and alternative (NM_203377, *MB-A*) *MB* transcripts were calculated by the standard curve approach measuring C_t values for hypoxic and normoxic samples ($n = 2$ experiments, triplicate assays). Differences in relative abundance between *MB-S* and *MB-A* transcripts in normoxic MDA-MB468 cells were calculated using the standard curve method and a standard plasmid construct harboring both amplicons, *MB-S* and *MB-A* ($n = 4$ experiments, duplicate assays).

Western Blots

Following normoxic exposure for 72 h and hypoxic (1% O_2) exposure for 4, 8, 24, 48, and 72 h, MDA-MB468 and MCF7 were harvested with a lysis buffer containing 0.1% Nonidet P-40, 400 mM NaCl, 1 mM EDTA (pH 8.0), 10 mM Tris-HCl (pH 8.0), and protease inhibitors. Protein extracts were electrophoresed on a 15% SDS-polyacrylamide gel. Primary antibodies (Abs) included the following: (*a*) monoclonal Ab (mAb) mouse anti-myoglobin (catalog no. 113-0533, clone Z001, Zytomed Systems GMBH, Berlin, Germany; dilution, 1:1000); (*b*) anti-

TABLE 1
Primers used for real time PCR and the generation of a HRE luciferase reporter construct (MluI and XhoI restriction enzyme recognition sites are underlined)

Gene	Primer sequence	Product size
		bp
Myoglobin	5′-GGCATCATGAGGCAGAGATT-3′ 5′-TCTGCAGAACCTGGATGATG-3′	111
MB-CDS	5′-GAGATGAAGGCGTCTGAGGA-3′ 5′-AACTACAAGGAGCTGGGCTTC-3′	294
GAPDH	5′-GAAGGTGAAGGTCGGAGTCA-3′ 5′-TGGACTCCACGACGTACTCA-3′	289
β-Actin	5′-GGACGACATGGAGAAAATC-3′ 5′-ATAGCACAGCCTGGATAGC-3′	185
MB-S (NM_005368)	5′-CCCAGTGAGCCCATACTTGC-3′ 5′-GTCAGAGGACGAGATGAAGGC-3′	219
MB-A (NM_203377)	5′-GCATGTTGGCCTGGTCCTTTGC-3′ 5′-GTCCTCATCAGGCTCTTTAAG-3′	275
L28 (NM_000991)	5′-GCAATTCCTTCCGCTACAAC-3′ 5′-TGTTCTTGCGGATCATGTGT-3′	198
HRE construct	5′-NNNNACGCGTTGGCATCCCCATGGCTTCT-3′ 5′-NNNNCTCGAGACCTCCAAAGGCCCATCTC-3′	376

HIF-1α mouse mAb (mgc3; 1:500); and (*c*) anti-HIF-2α rabbit polyclonal Ab (NB100-480, Novus Biologicals, LLC, Littleton; 1:750). For equal loading control, blots were stripped and reprobed by mAb mouse anti-β-actin at a 1:5000 dilution (A5441 Sigma).

Identification of Candidate Transcription Factor-binding Sites

Genomic sequences covering the analyzed gene loci were extracted from the NCBI database (www.ncbi.nlm.nih.gov) as follows: human *MB* (NC_000022), mouse *Mb* (NC_000081), and human *HSP27* (NC_000007). Putative transcription factor-binding sites conserved across different species were identified using the rVISTA program (32) whose searches utilize the TRANSFAC database (33). A global sequence alignment file as prepared by the program Mulan was used as input.

Functional Analysis of Candidate HRE via Dual-Luciferase Reporter Assays

A genomic region of 376 bp that included the candidate HRE was amplified from human placenta DNA (obtained from the Institute of Gynecology, University Hospital Mainz) using PCR primers listed in Table 1. The fragment was directionally cloned in a pGL3 promoter vector (Promega). MDA-MB468 cells were transfected using the FuGENE-HD reagent (Promega). For normalization of transfection efficiencies, all samples were co-transfected with a pGL4.74 vector. To investigate the influence of the candidate enhancer on the transcription efficiencies of the coding DNA sequence upon hypoxia, Dual-Luciferase reporter assays were performed at 72 h post-hypoxia exposure. Light signal quantification was measured in a Glomax 96-well luminometer (Promega), choosing a sample volume of 40 μl on both luciferin reagents ($n = 4$ experiments, triplicate assays). Standard deviations were calculated via Excel 2003 (Microsoft).

Stable and Transient RNA Interference

Targeting HIF—The following RNA oligonucleotides were synthesized to target the following: (*a*) nucleotides 1380–1400 of human HIF-1α mRNA (GenBank™ accession number AF304431.1) as sense 5′-CUGAUGACCAGCAACUUGAdTdT-3′ and antisense 5′-UCAAGUUGCUGGUCAUCAGdTdT-3′ sequences; (*b*) nucleotides 1260–1280 of human HIF-2α (GenBank™ accession number NM_001430) as sense 5′-CAGCAUCUUUGAUAGCAGUdTdT-3′ and antisense 5′-ACUGCUAUCAAAGAUGCUGdTdT-3′ sequences. Both siRNAs and the Si*CONTROL* nontargeting pool 2 of scrambled siRNAs were purchased from Dharmacon Research Inc. (Lausanne, Switzerland). 6-Well plate Oligofectamine transfections (Invitrogen) of siRNAs used final concentrations of 200 nM of either HIF-1α or -2α single siRNA and 100 nM each of HIF-1α and -2α siRNA in combined transfections.

Targeting MB—Short hairpin RNAs (shRNA) were used for targeting human *MB* mRNA (GenBank™ accession number NM_203377) at nucleotides 284–304 (construct 83), 483–503 (construct 84), 340–360 (construct 85), and 415–435 (construct 86). Inserted into the mammalian expression vector pLKO.1-puro, these four shRNA constructs were purchased as bacterial glycerol stock from Sigma. Stable shRNA MB knockdown MDA-MB468 cells were established by overnight calcium phosphate transfection followed by selection and maintenance in 0.75 μg/ml puromycin containing medium. For transient knockdown, MDA-MB468 cells were Lipofectamine-transfected (Invitrogen) with 20 (*i.e.* for knockdown 0–72 h) or 100 pmol (*i.e.* for knockdown 0–144 h) siRNA6 and -8 or all-Stars negative control scrambled RNA (Qiagen). Knockdown efficiency was confirmed on protein and/or RNA level using Western blot and real time quantitative PCR, respectively, as above.

High Resolution Respirometry

Oxygen kinetics of trypsinized, suspended, and heavily stirred MDA-MB468 cells, both of MB control and knockdown make up, were measured at $\sim 1 \times 10^6$/ml densities in twin-chamber Oroboros® Oxygraph-2k high resolution respirometers as summarized previously (34–36). Each chamber was filled with cells suspended in 2 ml of culture medium (glucose-free DMEM + 10% FBS + penicillin/streptomycin + 0.75 μg/ml puromycin). To measure routine respiration, the medium was initially free of glucose. Later, 25 mM glucose were added to measure the extent of its inhibition on respiration. To control oxygen levels and record sequentially replicated aerobic-anoxic transitions of respiratory activity of MDA-MB468 cells, injections of 40 μM H_2O_2 triggered the release of con-

trolled amounts of oxygen because the medium also contained 280 IU/ml catalase. Catalase dismutates rapidly hydrogen peroxide into oxygen and water such that the small amounts of added hydrogen peroxide do not induce any oxidative stress (37). For the recording of maximum oxygen flow as a measure of mitochondrial electron transfer capacity (ETS), oxidative phosphorylation was uncoupled with increasing doses (4.0–5.5 μM) of the protonophore carbonyl cyanide-4-(trifluoromethoxy)phenylhydrazone (FCCP). Finally, mitochondria were poisoned through injection of 0.5 μM myxothiazol to obtain the residual O_2 consumption (ROX). The oxygen partial pressure supporting half-maximal respiratory flux, $p_{50}(O_2)$, was calculated from aerobic-anoxic transitions in the routine state of respiration (with and without glucose in the medium), fitting a hyperbolic function between respiration (R) and oxygen pressure (pO_2) using the Hill equation,

$$R = R_{max} \cdot pO_2/(pO_2 + p_{50}) \quad \text{(Eq. 1)}$$

In Vitro Proliferation, Mitochondrial Activity and Migration Assays

Proliferation rates of wild type (WT) and selected stable MB-control or MB-knockdown (KD) MDA-MB468 clones was determined over a 96-h time course in normoxic and hypoxic atmospheres by direct counting of viable cells (trypan blue exclusion assay). In addition, we used the dimethylthiazolyldiphenyltetrazolium bromide (MTT) assay to infer viability from the colorimetric measurement of mitochondrial dehydrogenase activity in MDA-MB468 cells transfected with MB-silencing siRNA or scrambled (scr) control RNA oligonucleotides as a function of four different O_2 concentrations (normoxic atmosphere, 5, 1, and 0.2% O_2) over a 144-h time course.

In vitro motility of MDA-MB468 cells was assessed in transiently siRNA-transfected cells by performing a monolayer scratch wound assay at normoxic and hypoxic tensions (38). The wound closure dynamics was determined as percentage of remaining wound size by evaluation of the acellular gap width in relation to the initial wound width at three different sites for each wound in each picture (data as mean relative wound size ± S.D. of triplicate measurements/clone).

Statistical Analysis

Expression analysis (mRNA, protein), siRNA treatment, MTT assays, and respirometry results were analyzed using the package STATA 10.0 (Stata^{TM} 10.0; StataCorp., College Station, TX). Mean MB or CAIX mRNA and MB protein induction levels along a hypoxia time course (4, 8, 24, 48, 72 h, 1% O_2) were compared with basal abundance in normoxia controls (72 h). Also, MB induction was compared for corresponding time points between siControl *versus* siHIF-1α or siHIF-2α or the combined siHIF-1α/2α treatments. Mean O_2 consumption rates or p_{50} measurements were compared pairwise between pooled MB control and knockdown (KD) samples. Statistical significance was calculated by the following: (i) unpaired Student's t tests or one-way analysis of variance when normality of data population and variance equality among samples was ascertained (*e.g. MB* mRNA induction; MTT assay, scr *versus* si activity at same O_2 and time point; respirometry: R(-G), R(G), ROX O_2 consumption rates, all p_{50} data) or (ii) Welch-approximated t tests allowing unequal variances (*e.g.* MB protein induction; siRNA 72-h hypoxia time point comparison; ETS consumption rate). p values < 0.05 were considered significant.

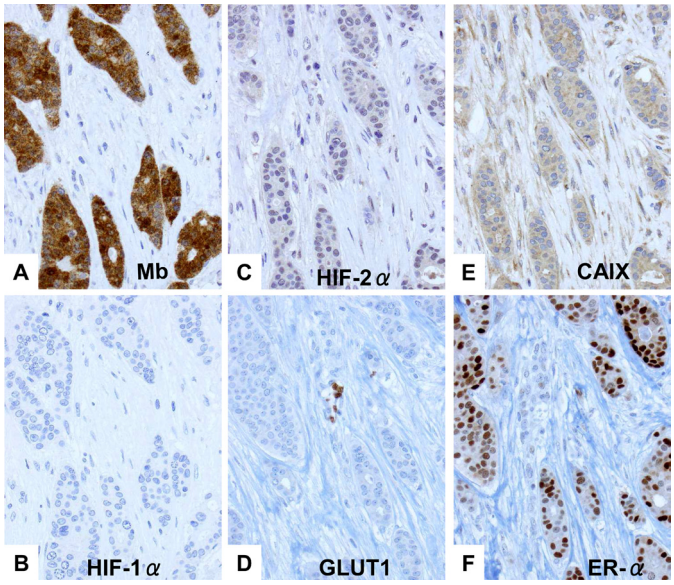

FIGURE 1. **Immunohistochemistry of MB, ERα, and endogenous markers of hypoxia in a typical case of moderately differentiated invasive ductal breast cancer.** *A,* cytoplasmic MB expression is abundant. *B,* lack of staining for HIF-1α. *C,* moderately positive staining (nuclear) for HIF-2α. *D,* lack of staining for GLUT1 (note erythrocytes staining in the center as internal positive control). *E,* moderately positive staining for CAIX. *F,* strong expression of estrogen receptor (ER)α.

RESULTS

We recently described that MB in breast cancer is positively and significantly correlated with estrogen (ERα), progesterone receptor, hypoxia-inducible factor-(HIF)-2α, and carbonic anhydrase IX (CAIX, Ref. 29). The typical expression profile of a MB-positive case is shown in Fig. 1 as follows: strong expression of MB and ERα, moderate but clearly discernible HIF-2α and CAIX expression, and weak expression or absence of HIF-1α and GLUT1. The positive correlation of MB with markers of tissue hypoxia (CAIX and HIF-2α) implied a possible control of MB expression by O_2. To clarify if MB expression also correlates with hypoxic tissue areas *in vivo*, we reanalyzed 137 cases of ductal carcinoma *in situ* (DCIS). DCIS represents an interesting *in vivo* model for hypoxia research because this tumor has no intraductal vasculature. Thus, ambient oxygen can only be supplied by diffusion across the outer basal membrane. This forms a radial O_2 diffusion gradient (normoxic rim; hypoxic to anoxic center) along with a central necrotic area (Fig. 2). Expression of the hypoxia-driven GLUT1 protein closely followed this gradient in our cohort of DCIS and showed a typical zonal distribution in 65% of cases (Fig. 2*A*). However, with regard to MB, only in 27% of MB-positive DCIS cases a hypoxia-like gradient with stronger staining in the peri-necrotic region was found (Fig. 2*A*). The majority of cases (73%) showed a diffuse MB immunoreactivity (Fig. 2*B*). This indicates that hypoxia may up-regulate MB *in vivo*, although in the majority of cases stimuli other than low pO_2 are driving the induction of MB. A similar conclusion was reached when we

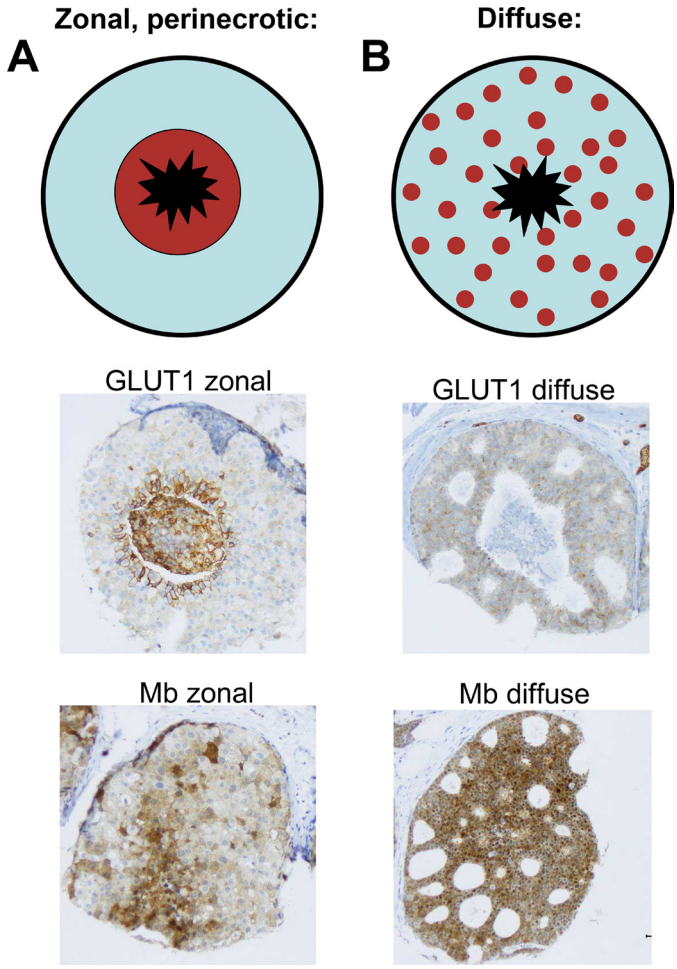

FIGURE 2. **DCIS as an *in vivo* model for tissue hypoxia.** The *upper panel* depicts DCIS schematically with a *black outer rim* (basal membrane), an inner zone (*light blue*) of atypical epithelial proliferates, and a central necrosis (*black star*). Expression of the hypoxia marker GLUT1 follows a zonal hypoxic gradient in 65% of DCIS cases (*A, middle*). However, also diffuse GLUT1 staining can be observed (*B, middle*). MB expression mostly displayed this diffuse staining (*B, bottom*) and showed the typical hypoxia-related zonal pattern in only 27% of cases (*A, bottom*).

assessed the possible co-localization between MB and hypoxic tumor areas as indicated by the hypoxia marker pimonidazole (supplemental Fig. S1).

We subsequently analyzed the responsiveness of the *MB* gene toward hypoxia (1% O_2) by quantitative PCR in the benign breast cell line MCF12A and three breast cancer cell lines (MDA-MB231, MDA-MB468, and MCF7). Although hypoxia did not affect the transcription of *MB* in benign MCF12A cells (supplemental Fig. S2), normalized steady state levels of *MB* mRNA increased 3–4-fold in hypoxic MDA-MB231 (data not shown), MDA-MB468, and MCF7 cells (Fig. 3*A*). For all cases, a significant activation of the *MB* gene required at least 24 or 48 h of hypoxia treatment. Proper hypoxic responsiveness of MCF7 cells was confirmed through assessment of transcription of the highly hypoxia-inducible CAIX transcript (Fig. 3*A*).

Of all examined breast cancer cell lines, MDA-MB468 cells contained the most abundant levels of *MB* transcripts under basal conditions (29). Superior abundance of MB in MDA-MB468 cells was also seen at a protein level (*i.e.* MDA-MB468, 65 ng of protein/10^6 cells (29); other breast cancer cell lines contain 24–32 ng of MB/10^6 cells (28)). Exceeding hypoxia (1% O_2) over 48 h (Fig. 3*B*) in MDA-MB-468 (*left panel*) and MCF7 cells (*right panel*) induced MB protein expression between 3.4- and 5.1-fold. The hypoxic response was transient when centered around HIF-1α (MCF7) or persistent (up to 72 h, 1% O_2) when HIF-2α acted as the predominant regulator (MDA-MB468) (Fig. 3*B*).

Next, the role of HIF in the hypoxic induction of MB was examined using HIF-1α and HIF-2α siRNA oligonucleotides. The siRNA assay focused on scrambled control and HIF-1α (= siHIF-1α), -2α (= siHIF-2α), and combined knockdown (KD) effects (= siHIF-1α/2α) after 52–96 h of exposure to 1% O_2 (Fig. 3*C*). Levels of MB steadily increased during siControl transfections to reach a maximal ~7-fold induction at 72 h of hypoxia (Fig. 3*C*). This peak induction was partially reduced upon HIF-1α or -2α single siRNA treatment. Yet the combination of both siRNAs yielded an ~20% residual amount of either HIF factor, which significantly attenuated the MB induction to ~1.7-fold at 72 h of hypoxia. In conclusion, this finding implies that both HIF-1 and HIF-2 participate in transactivating the *MB* gene by hypoxia.

To follow-up on this hypoxic transactivation of the *MB* gene by HIF-1/2, we compared the human *MB* gene locus to expressed sequence tags and detected the presence of several alternatively spliced *MB* transcripts in addition to the published mRNA (39). These transcript variants contain different non-coding 5′-untranslated regions (5′-UTRs) and hence are transcribed from different *MB* promoters (Fig. 4*A*). Comparison of expressed sequence tag numbers revealed that mRNA NM_005368 (NCBI-AceView Hsa *MB* variant B (40)) is the dominant "standard" transcript (*MB-S*) in muscle tissues of skeletal and heart. Transcript NM_203377 (NCBI-AceView Hsa *MB* variant D) was found encoded by the majority of cancer-associated expressed sequence tag reads. This mRNA (designated "*MB-A*" for "alternative") thus represented a candidate for analyzing its expression in breast cancer cells (Fig. 4*A*). Calculating the ratio of *MB-S versus MB-A* mRNA expression levels in normoxic MDA-MB468 breast cancer cells revealed a clear preference for *MB-A*, which was roughly 300-fold more abundantly expressed than *MB-S* (Fig. 4*B*). In MDA-MB468 cells subjected to either normoxia or 1% O_2 for 72 h, the steady state levels of *MB-S* were unaltered. On the contrary, the amount of *MB-A* transcripts increased 2.2-fold in hypoxic compared with normoxic cells. Using the rVISTA tool, we inspected the genomic regions of human and mouse *MB*/*Mb* genes for the presence of HIF-binding HREs, as characterized by the conserved consensus motif 5′-RCGTG-3′ (41). We detected one putative HRE at ~2.7 kb upstream of exon 1 (Fig. 4*A*), which consists of two inverted HIF-1-binding sites at an interval of 6 bp contained within a conserved stretch of 53 bp. This candidate *MB-HRE* has 92% sequence similarity to an upstream promoter region from the human heat shock protein *HSPB1* gene (Fig. 4*C*).

To investigate the functionality of the candidate HRE, Dual-Luciferase reporter assays were performed. MDA-MB468 cells were transfected with pGL3 promoter constructs that included a 376-bp section around the candidate HRE. 72 h post-hypoxia exposure, normalized luciferase activity was quantified in cell

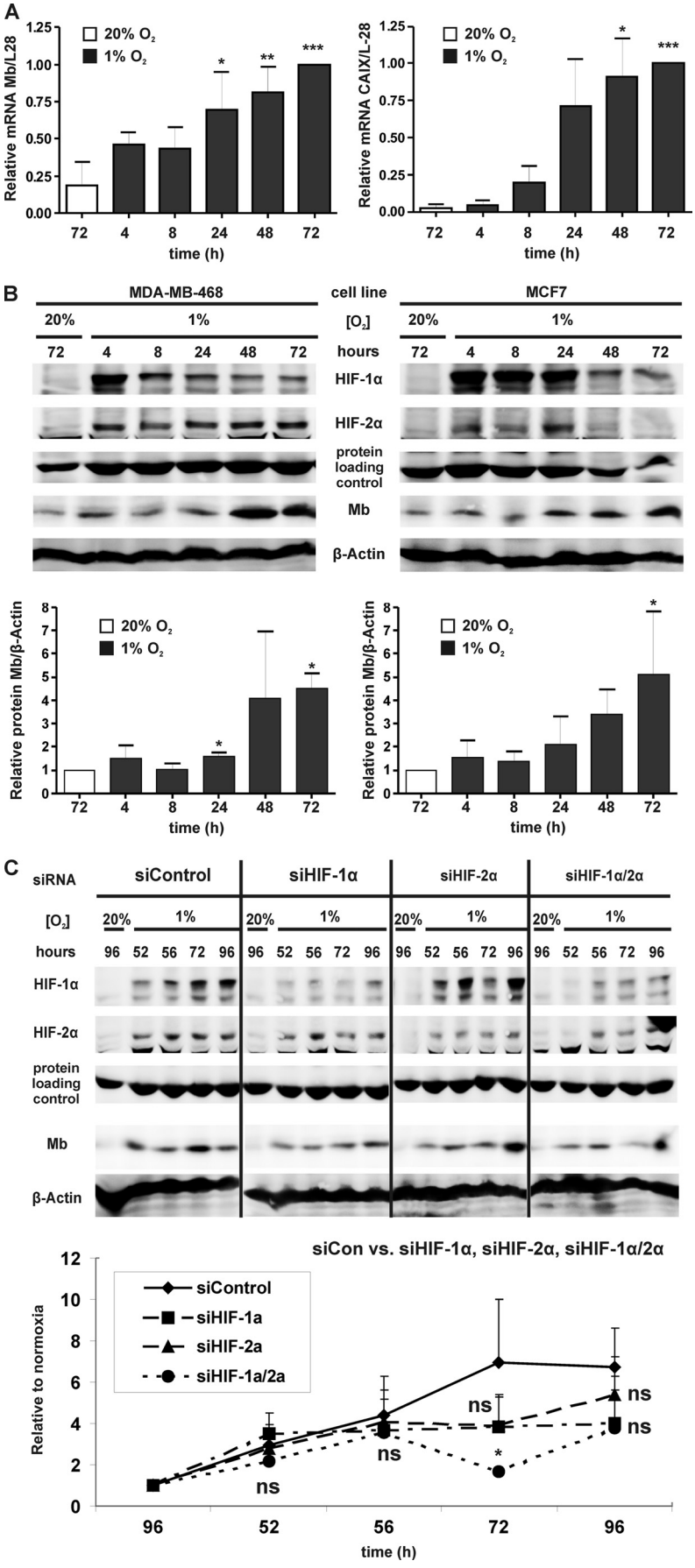
A
Relative mRNA Mb/L28
20% O2
1% O2
time (h)
Relative mRNA CAIX/L-28
B
MDA-MB-468
MCF7
cell line
[O2]
hours
HIF-1α
HIF-2α
protein loading control
Mb
β-Actin
Relative protein Mb/β-Actin
C
siRNA
siControl
siHIF-1α
siHIF-2α
siHIF-1α/2α
siCon vs. siHIF-1α, siHIF-2α, siHIF-1α/2α
siControl
siHIF-1a
siHIF-2a
siHIF-1a/2a
Relative to normoxia
ns

batches raised either under normoxic or hypoxic conditions (Fig. 4*D*). During hypoxia, the HRE-encoding construct showed an enhancer activity, which increased the amount of generated transcript by 43%, compared with the pGL3 promoter vector as a control. Under normoxia, no enhancer activity of the construct was observed.

To unravel functional properties of endogenous MB in breast cancer cells, we generated *stable* MB knockdown clones of MDA-MB468 cells using four different short hairpin (sh) RNA constructs (83–86). Applying Fick's law of diffusion, we aimed to see if the shRNA-mediated loss-of-function (LoF) of MB would yield a steeper oxygen diffusion gradient reflected by a higher $p_{50}(O_2)$ of cell respiration at identical oxygen flow. O_2 consumption kinetics were investigated by high resolution respirometry using two control clones (boxed, *84#5* and *85#14*) and two knockdown (KD) clones (boxed, *83#4* and *84#31*) (Fig. 5*A*). O_2 flow/s and million cells (*red tracing*) was recorded as a function of O_2 concentration (*blue tracing*) across four cellular activity states (Fig. 5*B*) as follows: (i) routine respiration without glucose (=*R*(-G)); (ii) routine respiration with 25 mM glucose (=*R*(G)); (iii) maximal respiration through uncoupling of oxidative phosphorylation by FCCP (=ETS); (iv) residual O_2 consumption after poisoning of mitochondria with myxothiazol (ROX). *R*(-G) and *R*(G) states indicate oxygen consumption at higher *versus* lower fluxes, respectively (Crabtree effect). To our surprise, all mitochondrial and residual O_2 fluxes were significantly increased in MB KD cells compared with control cells (Fig. 5*C*). In contrast, mean cellular cytochrome *c* oxidase $p_{50}(O_2)$ values (*i.e.* $p_{50}(O_2)$ of respiration) under *R*(-G) and *R*(G) conditions were statistically indistinguishable in control *versus* KD cell comparisons for either glucose-deficient or -proficient respiration (Fig. 5*D*). Differences in p_{50} values from high *versus* low oxygen fluxes were also nonsignificant.

We also investigated cellular proliferation during a 0-48-96-h time course in wild type (WT) and stable MB-CON and MB-KD MDA transfectants under both normoxic (*continuous lines*) and hypoxic (1% O_2, *hatched lines*) atmospheres by employing trypan blue-exclusion assays (Fig. 6*A*). MB LoF in stable knockdown transfectants yielded a significant diminishment of viable cells over the 96-h course, relative to WT cells or control transfectants, in both normoxic and hypoxic conditions.

Next, we assessed MDA-MB468 viabilities at normoxic and hypoxic pO_2 following siRNA-based *transient* silencing of MB expression to generate LoF phenotypes. This time we employed MTT assays during which mitochondrial dehydrogenases reduce a yellow tetrazolium substrate into a purple formazan compound as proxy for the oxidative capacity of living cells. Prior to the assay, cells were transfected with scrambled (scr) or MB-silencing siRNA (si) oligonucleotides. MTT reduction was followed over a 0-48-96-144 h time course as a function of four different O_2 concentrations: normoxia and 5, 1, or 0.2% O_2. Control RT-PCR analyses of MB mRNA expression ensured the Mb knockdown effect to last over the entire 144-h course (Fig. 6*B*, gel picture below *graph*). As expected, MTT conversion increased, because of continued cell and mitochondrial proliferation, linearly and with equivalent slopes over time in oxygenated cells (normoxia, 5% O_2), suggesting respiration of MDA-MB468 cells to operate in an oxyregulated fashion between 20 and 5% O_2. Compared with that, MTT conversion rose far less at 1% O_2 or was even ~2-fold inhibited during the time course at 0.2% O_2. Of note, pairwise comparisons of scr (*continuous lines* with *filled symbols*) *versus* MB-silencing treatments (*hatched lines* with *open symbols*) were, at the same O_2 conditions and time points, statistically indistinguishable in high oxygen (normoxia, 5% O_2) while revealing a borderline significant benefit of the MB knockdown on the activity of the MTT-converting mitochondrial enzymes in hypoxic cells (see scr/si *p* values at 0.2% O_2 course; Fig. 6*B*). 144 h si/scr ratios of MTT reduction rose steadily from near equality at 5% O_2 to a +18% (1% O_2) and, eventually, +46% (0.2% O_2) benefit in MB-silenced cells facing hypoxia (Fig. 6*B*).

Finally, we considered whether MB expression in breast cancer cells also influences the migration of normoxic or hypoxic cells on the basis of a scratch assay. As can be seen in Fig. 6, *C* and *D*, control cells (*i.e.* wild type MDA cells, either untreated or treated with scrambled RNA) were able to reconstitute the gap notably faster than MB KD cells treated with siRNA 6 or 8. This remarkable retardation of the *in vitro* motility in cells with repressed Mb expression established, especially after prolonged (48 h + 72 h) cultivation, a good agreement between loss of MB and impaired cellular migration potential in high and low pO_2.

DISCUSSION

To date, the existence of regional hypoxia in *most* solid tumors (for review see Refs. 42–45), including breast cancer (46), has been clearly established. Tumor hypoxia often associates with therapy resistance and poor prognosis. In accordance with Flonta *et al.* (28), we demonstrate *de novo* expression and hypoxic responsiveness of human MB mRNA and protein in human breast cancer cell lines. In contrast to nontransformed epithelial cells, malignant breast cancer cells induced both MB mRNA and protein 3–7-fold in response to prolonged exposure to 1% O_2. Peak induction of the MB protein in chronically

FIGURE 3. **MB expression in hypoxic breast cancer cells.** *A, MB* (*left*) and *CAIX* (*right*) mRNA expression during indicated times of hypoxia (1% O_2) in MCF7 cells (normalized expression, *MB/L28, CAIX/L28*; mean ± S.D., $n = 3$). Maximal mRNA abundance at 72 h of hypoxia was set to 1. Hypoxic *MB/L28* or *CAIX/L28* mRNA expressions (*black bars*) showing significantly elevated values ($p < 0.05$, <0.01, <0.001) relative to a basal steady state at 72 h normoxia (*white bar*) are indicated by 1–3 *asterisks*, respectively. *B,* protein expression of (top-to-bottom) HIF-1α, HIF-2α, MB, and β-actin in MDA-MB468 (*left*) and MCF7 (*right*) cells during indicated times of normoxia and hypoxia (1% O_2), respectively. *Lower bar graphs* show the densitometric summary of mean fold inductions (±S.D., $n = 3$) for normalized MB protein expression (*i.e.* MB/β-actin) during the hypoxia time course relative to the proteins normoxic levels (= 1) for MDA-MB468 (*left*) and MCF7 (*right*) cells. Hypoxic inductions (*black bars*) showing significantly elevated values ($p < 0.05$) relative to basal MB levels at 72 h of normoxia (*white bars*) are indicated by *single asterisks*. *C,* transfection of MDA-MB468 cells with scrambled RNA (siControl) or HIF-1α and HIF-2α transcript-targeting siRNAs. Representative Western blots show (*top-to-bottom*) HIF-1α, HIF-2α, MB, and β-actin protein abundance for 96 h of normoxia *versus* 52, 56, 72, and 96 h of hypoxia (1% O_2). The protein loading control is shown in the *middle*. *Bottom graph,* corresponding MB protein fold inductions (mean ± S.D.; $n = 3$) during indicated hypoxia times are plotted relative to 96 h normoxia (set to 1). Relative to the siControl value at a given time point, siHIF-1α, siHIF-2α, and siHIF-1α/2α values of MB content were nonsignificantly (*ns*) or significantly different (*, $p < 0.05$).

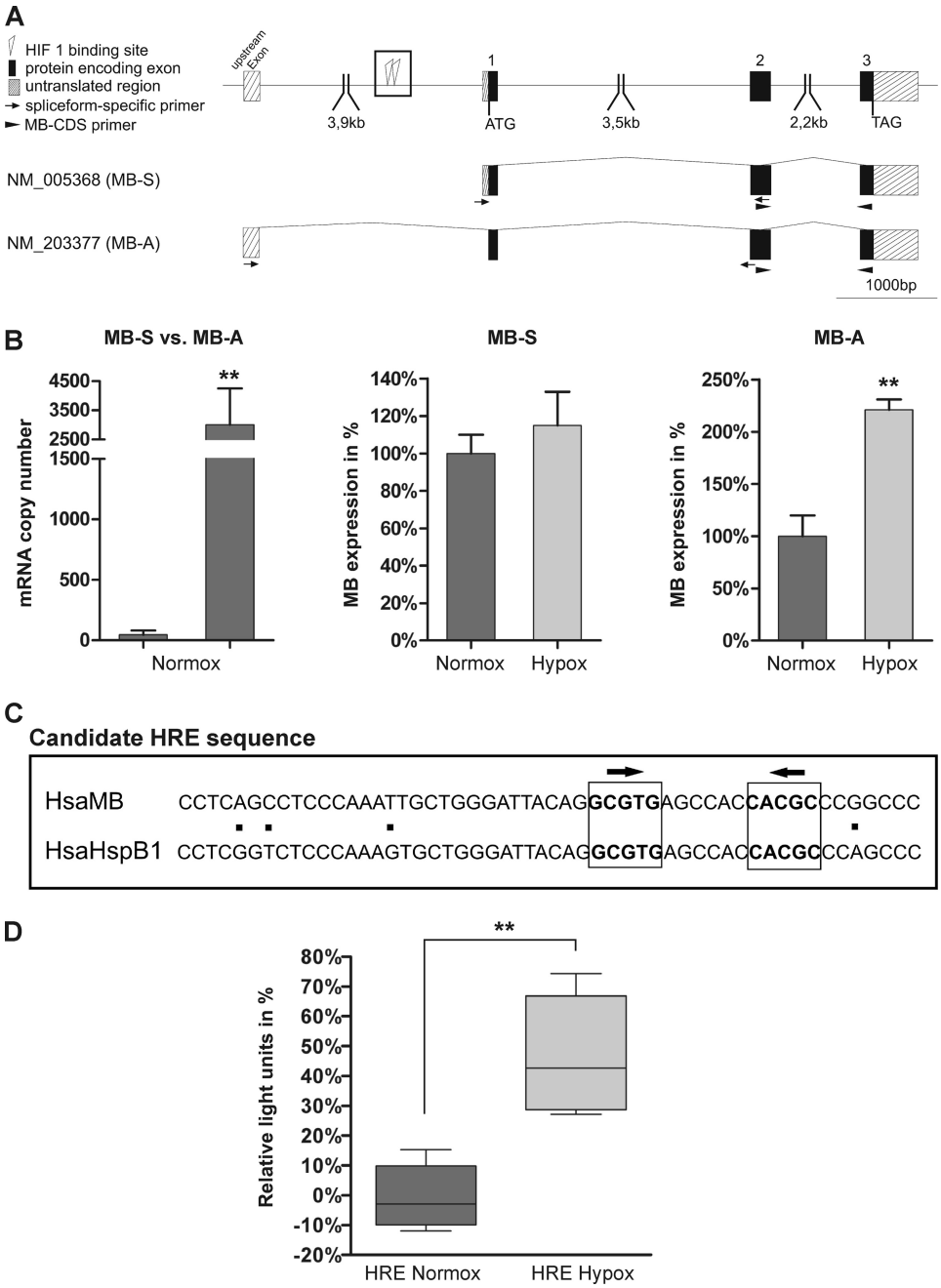

FIGURE 4. **Hypoxia induction of alternative MB transcripts.** *A,* schematic overview of the Hsa *MB* gene structure, the *MB* standard transcript NM_005368 (*MB-S*), and an alternative transcript variant NM_203377 (*MB-A*). Protein encoding exons are indicated by *black boxes*, and untranslated exonic regions are *hatched*. Positions of PCR primers that specifically amplify *MB* mRNA isoforms are indicated by *arrows*. PCR primers for measuring total *MB* mRNA levels matched the *MB* coding sequence (*CDS* primers, *filled arrowheads*). *Open box,* a candidate HRE, which consists of two HIF-1-binding sites in inverted orientation (*triangles*). *B, left,* mRNA quantification of the *MB-S* transcript compared with the *MB-A* transcript variant in MDA-MB-468 cells cultured under normoxic conditions (**, $p < 0.01$; $n = 4$). *Middle* and *right,* differential expression of the transcripts *MB-S* and *MB-A* in hypoxic (*Hypox*) *versus* normoxic (*Normox*) MDA-MB-468 cells (**, $p < 0.01$; $n = 4$). *C,* sequence of the candidate *MB* HRE. Alignment of a 53-bp region (see *open box* in *A*) conserved between the Hsa *MB* gene and the *HspB1* gene. Two potential HIF-1-binding sites of inverted orientation (*arrows*) are printed in *boldface*. *D,* luciferase reporter assays show that the candidate HRE features enhancer activity in hypoxic MDA-MB468 cells, compared with normoxic samples. Box plots present the range of minimal-maximal samples (lower/upper whisker), the 25% (Q1) to 75% (Q3) quartiles (*box*), and the median (*line in box*) (**, $p < 0.01$; $n = 4$).

hypoxic MDA-MB468 cells further required the involvement of HIF-1 and HIF-2 protein. We further noted that the standard TATA box promoter of both human and mouse *MB/Mb* genes (39, 47), which drives the expression in striated muscle cells, lacks candidate HREs (17). Consequently, we found expression of the standard *MB* transcript (NM_005368; *MB-S*) to not be affected by O_2. However, a noncanonical *MB* mRNA (NM_203377; *MB-A*), transcribed from a novel promoter proximal to the 5′-UTR upstream exon, greatly exceeded in MDA-MB468 cells the copy numbers of the *MB-S* mRNA, suggesting that *MB-A*, tentatively, can be regarded as a cancer-specific transcript. Discovery of the O_2 responsiveness of *MB-A*, in conjunction with the found HIF-1/2-driven transactivation of the *MB* gene during hypoxia, was backed by the presence of a can-

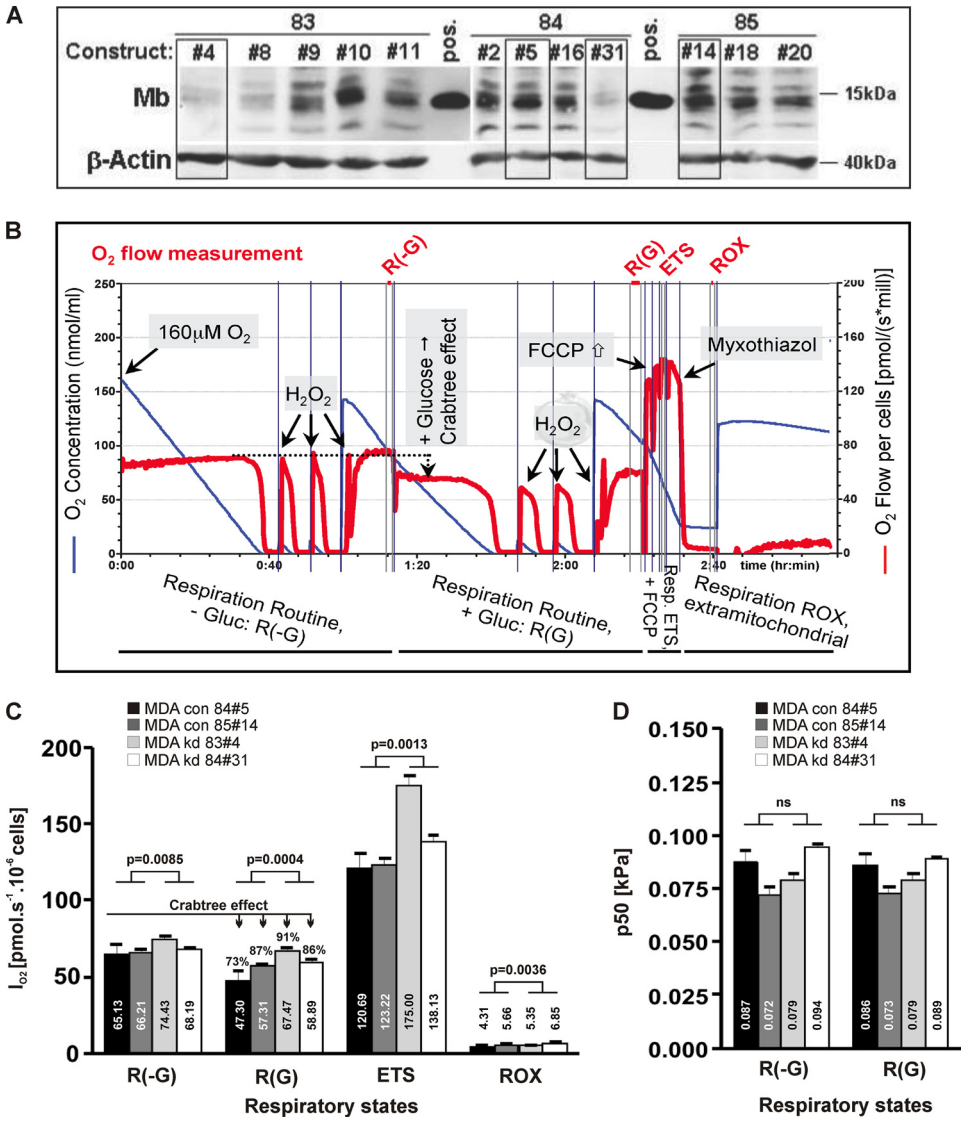

FIGURE 5. **High resolution respirometry of control and MB knockdown MDA-MB468 cells.** *A,* MB and β-actin Western blot of 12 MDA-MB-468 shRNA clones, derived from shRNA constructs 83, 84, and 85, together with positive (*pos.*) MB control extractions from a human skeletal muscle biopsy. MB control (*84#5, 85#14*) and knockdown (*83#4, 84#31*) clones used for respirometry are *boxed*. *B,* original MDA-MB-468 cell respirometry shown as O_2 flow/s and million cells (*red tracing*) as a function of O_2 concentration (*blue tracing*) across four cellular activity states as follows: routine respiration without/with glucose (*R*(-G), *R*(G)); maximal respiration through uncoupling of oxidative phosphorylation by FCCP (= ETS); residual O_2 consumption after poisoning of mitochondria with myxothiazol (=ROX) (see under "Experimental Procedures" for more details). *C,* O_2 consumption rates of MB control (*con*; *black* + *dark gray column*) and MB knockdown clones (*kd*; *light gray* + *white column*) for the *R*(-G), *R*(G), ETS, and ROX states. *D,* oxygen kinetic $p_{50}(O_2)$ data of respiration in MB control (*black* + *dark gray column*) and MB KD clones (*light gray* + *white column*) for *R*(-G) and *R*(G) states. Mean $p_{50}(O_2)$ values are highlighted within the respective column.

didate HRE at ~2.7 kb upstream of exon 1 of the *MB* gene. The motif consists of two inverted HIF-1-binding sites at an interval of 6 bp, embedded in a conserved stretch of 53 bp. This MB-HRE has 92% sequence similarity to an upstream promoter region from the HSP27 human heat shock protein encoding gene *HSPB1*, which was reported to house a functional and HIF-1 binding HRE (48). Our preliminary analysis indicates that this MB-HRE features an enhancer activity of 43% upon exposure to hypoxia.

Based on these findings, we assume that breast cancer cells induce *MB* in response to longer periods of low oxygen via an alternative and perhaps tumor-specific promoter whose enhanced activity might be also dependent on the binding of HIF-1/2 to the HRE located 2.7 kb upstream of the genuine ATG. The statistically significant positive correlation of MB with HIF-2α and CAIX in breast carcinomas further points toward mechanistic networking of these factors under hypoxia. However, our *in vivo* data also provide evidence that MB can be expressed by breast epithelia irrespective of hypoxia (29) and that even severe hypoxia in pimonidazole-stained carcinoma does not necessarily trigger MB induction (supplemental Fig. S1).

MB has multiple known or alleged functions in muscle tissue, including short term O_2 storage and buffering, facilitating O_2 diffusion, scavenging of NO and reactive oxygen species and also the reverse (peroxidase activity, NO production), and the binding plus transport of fatty acids (2–4, 6–11, 49). To assess whether MB also confers O_2-buffering or facilitates O_2 diffusion in cancer cells, we used high resolution respirometry to measure O_2 consumption kinetics in MB expressing control

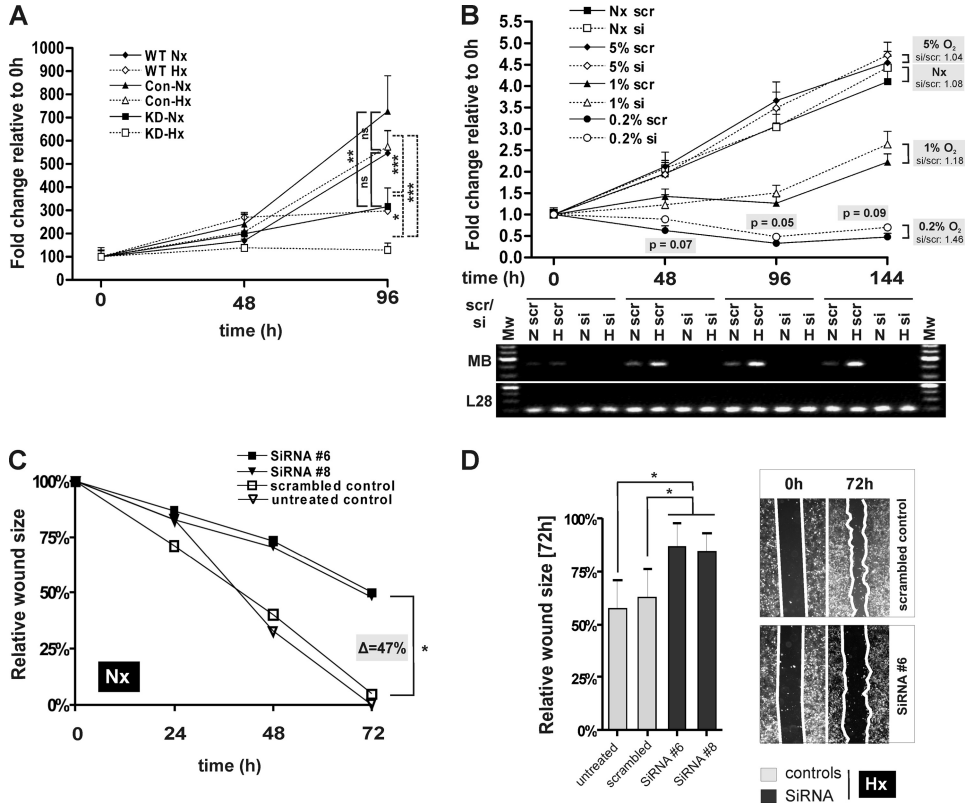

FIGURE 6. **Functional analysis of MB knockdown effects.** *A,* proliferation assay by trypan blue exclusion. Counts of viable cells were computed over a 0–48-96 h time course of wild type (*WT*, *diamonds*), MDA-MB-468 cells and stable MB-control (*CON*, *triangles*), and MB-knockdown (*KD*, *squares*) clones under normoxic (*continuous lines*) and hypoxic (1% O_2, *hatched lines*) conditions. Data (mean ± S.D., $n = 3$) are given in %, relative to 0 h = 100%. *B,* MTT viability assay. Following transfection with scrambled control (*scr*) or *MB*-silencing siRNA oligonucleotides (*si*), MDA-MB468 cells were subjected to a 0–48-96–144-h time course at four different O_2 concentrations (normoxia; 5% O_2, 1% O_2, 0.2% O_2). Given are mean (±S.E., $n = 4$) MTT conversion activities in fold changes relative to the 0-h time point (=1). Note the correlation between atmospheric O_2 content and progressive delay of benefit from the *MB* knockdown (*i.e.* shifting of si-MTT > scr-MTT activity crossover points for 0.2% → 1% → 5%, normoxia (*Nx*) to later time points). Gel picture *below graph*: representative control RT-PCR of *MB* and ribosomal protein *L28* (loading control) mRNA expression at normoxic (*N*) and 1% O_2 hypoxic (*H*) exposures for indicated time points, in presence of scrambled (*scr*) or *MB* silencing (*si*) oligonucleotides. Note the *MB* knockdown effect to last over the entire 144-h course and *MB* mRNA induction at 1% O_2 at 48-, 96-, and 144-h time points (scr treatment). *C* and *D,* scratch assay for investigating cell motility. Confluent MDA-MB-468 cells were scratched with a pipette tip, and the size of the gap was evaluated after 24, 48, and 72 h at normoxia (*Nx*, *C*) or 72 h at hypoxia (*Hx*, *D*). Diagrams of wound closure over time indicate cell migration capacity. Results are averages of triplicate experiments for each approach.

and KD MDA-MB468 cells, expecting the latter to develop higher intracellular oxygen gradients (reflected by a higher $p_{50}(O_2)$ of cell respiration at identical oxygen flow) than controls. Because facilitated diffusion of oxygen can only occur when MB is partially desaturated with oxygen, the above prediction of Fick's law of diffusion was carefully assessed with $pO_2 \leq 1.1$ to 0 kPa (= 8.3 to 0 mm Hg; see *blue tracing* of [O_2] in Fig. 5*B* and note development of controlled amounts of oxygen by H_2O_2 injections into catalase-containing medium to generate replicate aerobic-anoxic transitions and thus a more accurate determination of $p_{50}(O_2)$ of cell respiration (37)). With the 37 °C half-saturation (Y_{50}) of MB occurring at pO_2 of 2.4 mm Hg (50), a transition from 1.1 to 0 kPa corresponds to a fractional O_2 saturation of MB ranging from ~78% to complete deoxygenation (see under "Experimental Procedures" for details). Although our respirometric conditions were well suited to trigger MB into O_2 unloading and to potentially detect any facilitated O_2 diffusion, it needs to be stressed that $p_{50}(O_2)$ measures of respiration of small cells and isolated mitochondria usually are below 0.1 kPa (51). Thus, only a small scope for intracellular oxygen gradients exists (51). Within these physical constraints, this study was unable to provide any evidence for O_2 gradients that are differentially influenced by the presence or absence of MB protein. In fact, the $p_{50}(O_2)$ of MB-CON and -KD MDA-MB468 cells was found to lie in a similar range (0.08 kPa). These results do not suggest a functional role of MB in oxygen transport in small, suspended cells *in vitro*. However, they do not exclude the possibility of larger oxygen gradients developing in the solid tumor and a potential contribution of MB to facilitated oxygen diffusion under *in vivo* conditions. Furthermore, routine respiration in MDA-MB468 cells was activated ~55% (*i.e.* *R*(-G)) and ~40% (*i.e.* *R*(G)), respectively, of the mitochondrial capacity for electron transfer (ETS), which is comparable with various primary cultured cells such as human umbilical vein endothelial cells and fibroblasts (34, 52, 53). Mitochondrial oxygen kinetics and coupling control in malignant MDA-MB468 cells is therefore not indicative of a mitochondrial deficiency frequently considered as a specific feature (Warburg effect) of cancer cells.

In addition to these respirometry data from O_2-limiting hypoxia, we also noticed the intensified O_2 uptake rate across all four physiological activity states considered (*R*(-G), *R*(G), ETS, ROX) by MDA knockdown cells during mild hypoxia. As a hemoprotein, MB can effectively interact with the gaseous

nitric oxide (NO). MB knock-out mouse models (1, 5) have been instrumental to elicit the critical role of MB in maintaining NO homeostasis in muscle tissue. Whether MB expressed in neoplasms exerts similar controls remains to be seen. At this point, we can only speculate that the respiratory activation and enhancement of substrate turnover by MTT-converting mitochondrial dehydrogenases, both noted for hypoxic MDA cells in response to MB LoF, might result from the capacity of the oxygenated fraction of MB (*i.e.* MBO_2) to scavenge NO (*i.e.* $NO + MBO_2 \rightarrow metMB + NO_3^-$), a key stimulus of mitochondrial biogenesis (54). Alternatively, the presence of MB may also exert some oxidative stress (*i.e.* bound O_2 is released as reactive oxygen species) particularly during stages of hypoxia, and in that way act to inhibit mitochondrial activity. Our results on oxygen kinetics, however, suggest that MB does not play a detectable role in regulating levels of NO that inhibit oxidative phosphorylation (OXPHOS) in suspended breast cancer cells. Using inducible NOS-transfected HEK293 cells to achieve regulated intracellular NO production, however, demonstrated that nanomolar concentrations of NO could trigger an increase of low $p_{50}(O_2)$ (*i.e.* <0.1 kPa) values by 2 orders of magnitude, which underpinned the tight coupling between NO homeostasis and O_2 consumption kinetics in this cell model (55).

So far only two studies have analyzed the potential roles of myoglobin in nonmuscle contexts by employing artificial expression systems. Nitta *et al.* (56) induced MB expression in hepatocytes by an adenoviral gene transfer, which were henceforth significantly more resistant to hypoxia. Galluzzo *et al.* (57) were the first to introduce abundant levels of mouse Mb into the human tumor cell line A549 (lung carcinoma) by lentiviral gene transfer. Experimental tumors expressing ectopic Mb displayed reduced or no hypoxia, minimal HIF-1α levels, lower vessel density along with a more differentiated cancer cell phenotype, and largely suppressed local and distal metastatic spreading. The authors correlated these beneficial outcomes of Mb overexpression primarily with the reduction of tumor hypoxia (57). Although these findings appear to match our *in vivo* observation from patients, where patients with higher MB levels show a better prognosis (29), both situations are quite different. First, the low quantities of endogenous MB measured by us in normoxic MDA-MB468 breast cancer cells ($\sim$65 ng of MB protein/10^6 cells) cannot confer meaningful O_2 storage/buffering capacity. Second, our respirometry data failed to provide evidence for a functional role of MB in the transport of oxygen *in vitro*. Finally, at least in hypoxic breast cancer cells, MB has an interfering (*i.e.* not promoting) impact on O_2 uptake and oxidative energy metabolism, which suggests a tumor-suppressive function of MB in deoxygenated malignancies. These fundamental discrepancies require, in our opinion, a cautionary note when overexpression-based molecular evidence is directly interpreted in terms of endogenous protein functions.

In summary, MB abundance in breast cancer cells is regulated not only by estrogen signaling and possibly fatty acid levels or growth factors but also by hypoxia (29). The intensified respiration and mitochondrial enzyme activities in hypoxic cancer cells in response to a silencing of MB expression might either result from mitochondrial compensation(s) (*e.g.* increase in mitochondrial density/size because of NO overabundance) or, perhaps, reflect a higher level of oxidative stress exerted by the presence of this hemoprotein. The fact that MB LoF yields declining proliferation or motility rates even in fully oxygenated cells suggests MB in cancer cells to occupy rather unconventional functions that are not directly related to the binding and transport of O_2. By acting as a putative shuttle for fatty acids, MB could possibly support active lipogenesis and cellular growth even at times when the O_2 supply is nonlimiting and the protein is in its fully O_2-saturated state (*i.e.* MBO_2). Beyond these functional aspects, the regulation in normal and tumor tissue might also be fundamentally different, as the novel description of a tumor-specific *MB* transcript suggests. Together, these findings further broaden our view on the role of nonmuscle MB that may have fundamental implications for our conception of the biology of solid tumors.

Acknowledgments—The excellent technical assistance of Martina Storz, Silvia Behnke, and Sonja von Serenyi is gratefully acknowledged. We thank Dr. Peter Uciechowski (RWTH Aachen, Germany) for giving us access to the hypoxia workstation.

REFERENCES

1. Gödecke, A., Flögel, U., Zanger, K., Ding, Z., Hirchenhain, J., Decking, U. K., and Schrader, J. (1999) *Proc. Natl. Acad. Sci. U.S.A.* **96,** 10495–10500
2. Ordway, G. A., and Garry, D. J. (2004) *J. Exp. Biol.* **207,** 3441–3446
3. Wittenberg, J. B. (1970) *Physiol. Rev.* **50,** 559–636
4. Jürgens, K. D., Peters, T., and Gros, G. (1994) *Proc. Natl. Acad. Sci. U.S.A.* **91,** 3829–3833
5. Garry, D. J., Ordway, G. A., Lorenz, J. N., Radford, N. B., Chin, E. R., Grange, R. W., Bassel-Duby, R., and Williams, R. S. (1998) *Nature* **395,** 905–908
6. Flögel, U., Merx, M. W., Gödecke, A., Decking, U. K., and Schrader, J. (2001) *Proc. Natl. Acad. Sci. U.S.A.* **98,** 735–740
7. Hendgen-Cotta, U. B., Merx, M. W., Shiva, S., Schmitz, J., Becher, S., Klare, J. P., Steinhoff, H. J., Göedecke, A., Schrader, J., Gladwin, M. T., Kelm, M., and Rassaf, T. (2008) *Proc. Natl. Acad. Sci. U.S.A.* **105,** 10256–10261
8. Khan, K. K., Mondal, M. S., Padhy, L., and Mitra, S. (1998) *Eur. J. Biochem.* **257,** 547–555
9. Flögel, U., Gödecke, A., Klotz, L. O., and Schrader, J. (2004) *FASEB J.* **18,** 1156–1158
10. Sriram, R., Kreutzer, U., Shih, L., and Jue, T. (2008) *FEBS Lett.* **582,** 3643–3649
11. Tomita, A., Kreutzer, U., Adachi, S., Koshihara, S. Y., and Jue, T. (2010) *J. Exp. Biol.* **213,** 2748–2754
12. Reynafarje, B. (1962) *J. Appl. Physiol.* **17,** 301–305
13. Vogt, M., Puntschart, A., Geiser, J., Zuleger, C., Billeter, R., and Hoppeler, H. (2001) *J. Appl. Physiol.* **91,** 173–182
14. Wittenberg, B. A. (2009) *Am. J. Physiol. Cell Physiol.* **296,** C390–C392
15. Ameln, H., Gustafsson, T., Sundberg, C. J., Okamoto, K., Jansson, E., Poellinger, L., and Makino, Y. (2005) *FASEB J.* **19,** 1009–1011
16. Chang, H., Shyu, K. G., Wang, B. W., and Kuan, P. (2003) *Clin. Sci.* **105,** 447–456
17. Wystub, S., Ebner, B., Fuchs, C., Weich, B., Burmester, T., and Hankeln, T. (2004) *Cytogenet. Genome Res.* **105,** 65–78
18. Fordel, E., Geuens, E., Dewilde, S., De Coen, W., and Moens, L. (2004) *IUBMB Life* **56,** 681–687
19. Kanatous, S. B., Mammen, P. P., Rosenberg, P. B., Martin, C. M., White, M. D., Dimaio, J. M., Huang, G., Muallem, S., and Garry, D. J. (2009) *Am. J. Physiol. Cell Physiol.* **296,** C393–C402
20. Fraser, J., de Mello, L. V., Ward, D., Rees, H. H., Williams, D. R., Fang, Y., Fang, Y., Brass, A., Gracey, A. Y., and Cossins, A. R. (2006) *Proc. Natl. Acad. Sci. U.S.A.* **103,** 2977–2981
21. Roesner, A., Mitz, S. A., Hankeln, T., and Burmester, T. (2008) *FEBS J.* **275,**

3633–3643
22. Enoki, Y., Morimoto, T., Nakatani, A., Sakata, S., Ohga, Y., Kohzuki, H., and Shimizu, S. (1988) *Adv. Exp. Med. Biol.* **222,** 709–716
23. Qiu, Y., Sutton, L., and Riggs, A. F. (1998) *J. Biol. Chem.* **273,** 23426–23432
24. Eusebi, V., Bondi, A., and Rosai, J. (1984) *Am. J. Surg. Pathol.* **8,** 51–55
25. Smith, T. W., and Davidson, R. I. (1984) *Cancer* **54,** 323–332
26. Iseki, M., Tsuda, N., Kishikawa, M., Shimada, O., Hayashi, T., Kawahara, K., and Tomita, M. (1990) *Am. J. Surg. Pathol.* **14,** 395–398
27. Zhang, P. J., Goldblum, J. R., Pawel, B. R., Fisher, C., Pasha, T. L., and Barr, F. G. (2003) *Mod. Pathol.* **16,** 229–235
28. Flonta, S. E., Arena, S., Pisacane, A., Michieli, P., and Bardelli, A. (2009) *Am. J. Pathol.* **175,** 201–206
29. Kristiansen, G., Rose, M., Geisler, C., Fritzsche, F. R., Gerhardt, J., Lüke, C., Ladhoff, A. M., Knüchel, R., Dietel, M., Moch, H., Varga, Z., Theurillat, J. P., Gorr, T. A., and Dahl, E. (2010) *Br. J. Cancer* **102,** 1736–1745
30. Gorr, T. A., Wichmann, D., Pilarsky, C., Theurillat, J. P., Fabrizius, A., Laufs, T., Bauer, T., Koslowski, M., Horn, S., Burmester, T., Hankeln, T., and Kristiansen, G. (2011) *Acta Physiologica* **202,** 563–581
31. Wirthner, R., Wrann, S., Balamurugan, K., Wenger, R. H., and Stiehl, D. P. (2008) *Carcinogenesis* **29,** 2306–2316
32. Loots, G. G., and Ovcharenko, I. (2004) *Nucleic Acids Res.* **32,** W217–W221
33. Wingender, E., Chen, X., Hehl, R., Karas, H., Liebich, I., Matys, V., Meinhardt, T., Prüss, M., Reuter, I., and Schacherer, F. (2000) *Nucleic Acids Res.* **28,** 316–319
34. Steinlechner-Maran, R., Eberl, T., Kunc, M., Margreiter, R., and Gnaiger, E. (1996) *Am. J. Physiol.* **271,** C2053–C2061
35. Gnaiger, E., Steinlechner-Maran, R., Méndez, G., Eberl, T., and Margreiter, R. (1995) *J. Bioenerg. Biomembr.* **27,** 583–596
36. Gnaiger, E. (2001) *Respir. Physiol.* **128,** 277–297
37. Pesta, D., and Gnaiger, E. (2011) in *Mitochondrial Bioenergetics: Methods and Protocols* (Palmeira, C., and Moreno, A., eds) Humana Press, New York
38. Rosman, D. S., Phukan, S., Huang, C. C., and Pasche, B. (2008) *Cancer Res.* **68,** 1319–1328
39. Weller, P., Jeffreys, A. J., Wilson, V., and Blanchetot, A. (1984) *EMBO J.* **3,** 439–446
40. Thierry-Mieg, D., and Thierry-Mieg, J. (2006) *Genome Biol.* **7,** Suppl. 1, S12, 1–14
41. Wenger, R. H., Stiehl, D. P., and Camenisch, G. (2005) *Sci. STKE 2005,* re12
42. Vaupel, P., Schlenger, K., Knoop, C., and Höckel, M. (1991) *Cancer Res.* **51,** 3316–3322
43. Thews, O., Koenig, R., Kelleher, D. K., Kutzner, J., and Vaupel, P. (1998) *Br. J. Cancer* **78,** 752–756
44. Brown, J. M. (1999) *Cancer Res.* **59,** 5863–5870
45. Brown, J. M., and Wilson, W. R. (2004) *Nat. Rev. Cancer* **4,** 437–447
46. Arcasoy, M. O., Amin, K., Karayal, A. F., Chou, S. C., Raleigh, J. A., Varia, M. A., and Haroon, Z. A. (2002) *Lab. Invest.* **82,** 911–918
47. Blanchetot, A., Price, M., and Jeffreys, A. J. (1986) *Eur. J. Biochem.* **159,** 469–474
48. Whitlock, N. A., Agarwal, N., Ma, J. X., and Crosson, C. E. (2005) *Invest. Ophthalmol. Vis. Sci.* **46,** 1092–1098
49. Wittenberg, B. A., Wittenberg, J. B., and Caldwell, P. R. (1975) *J. Biol. Chem.* **250,** 9038–9043
50. Schenkman, K. A. (2001) *Am. J. Physiol. Heart Circ. Physiol.* **281,** H2463–H2472
51. Scandurra, F. M., and Gnaiger, E. (2010) *Adv. Exp. Med. Biol.* **662,** 7–25
52. Hutter, E., Renner, K., Pfister, G., Stöckl, P., Jansen-Dürr, P., and Gnaiger, E. (2004) *Biochem. J.* **380,** 919–928
53. Smolková, K., Bellance, N., Scandurra, F., Génot, E., Gnaiger, E., Plecitá-Hlavatá, L., Jezek, P., and Rossignol, R. (2010) *J. Bioenerg. Biomembr.* **42,** 55–67
54. Nisoli, E., Clementi, E., Carruba, M. O., and Moncada, S. (2007) *Circ. Res.* **100,** 795–806
55. Aguirre, E., Rodríguez-Juárez, F., Bellelli, A., Gnaiger, E., and Cadenas, S. (2010) *Biochim. Biophys. Acta* **1797,** 557–565
56. Nitta, T., Xundi, X., Hatano, E., Yamamoto, N., Uehara, T., Yoshida, M., Harada, N., Honda, K., Tanaka, A., Sosnowski, D., Chance, B., and Yamaoka, Y. (2003) *J. Surg. Res.* **110,** 322–331
57. Galluzzo, M., Pennacchietti, S., Rosano, S., Comoglio, P. M., and Michieli, P. (2009) *J. Clin. Invest.* **119,** 865–875